Published in final edited form as:
Toxicol Mech Methods. 2016 June ; 26(5): 362–370. doi:10.1080/15376516.2016.1190991.

Connexin32 deficiency exacerbates carbon tetrachloride-induced hepatocellular injury and liver fibrosis in mice

Bruno Cogliati[#1,*], **Sara Crespo Yanguas**[#2], **Tereza C. da Silva**[1], **Thiago P.A. Aloia**[1], **Marina S. Nogueira**[3], **Mirela A. Real-Lima**[1], **Lucas M. Chaible**[1], **Daniel S. Sanches**[1], **Joost Willebrords**[2], **Michaël Maes**[2], **Isabel V.A. Pereira**[1], **Inar A. de Castro**[3], **Mathieu Vinken**[2,†], and **Maria L.Z. Dagli**[1,†]

[1]Department of Pathology, School of Veterinary Medicine and Animal Science, University of Sao Paulo, Sao Paulo, Brazil

[2]Department of *In Vitro* Toxicology and Dermato-Cosmetology, Vrije Universiteit Brussel, Brussels, Belgium

[3]Department of Food and Experimental Nutrition, Faculty of Pharmaceutical Sciences, University of São Paulo, São Paulo, Brazil

[#] These authors contributed equally to this work.

Abstract

Background and aims—Liver fibrosis results from the perpetuation of the normal wound healing response to several types of injury. Despite the wealth of knowledge regarding the involvement of intracellular and extracellular signaling pathways in liver fibrogenesis, information about the role of intercellular communication mediated by gap junctions is scarce.

Methods—In this study, liver fibrosis was chemically induced by carbon tetrachloride in mice lacking connexin32, the major liver gap junction constituent. The manifestation of liver fibrosis was evaluated based on a series of read-outs, including fibrosis staging and collagen morphometric analysis, oxidative stress, apoptotic, proliferative and inflammatory markers.

Results—More pronounced liver damage and enhanced collagen deposition were observed in connexin32 knock-out mice compared to wild-type animals in experimentally triggered induced liver fibrosis. No differences between both groups were noticed in apoptotic signaling nor in inflammation markers. However, connexin32 deficient mice displayed decreased catalase activity and increased malondialdehyde levels.

Conclusions—These findings could suggest that connexin32-based signaling mediates tissue resistance against liver damage by the modulation of the anti-oxidant capacity. In turn, this could point to a role for connexin32 signaling as a therapeutic target in the treatment of liver fibrosis.

[*]Corresponding author at University of São Paulo, School of Veterinary Medicine and Animal Science, Department of Pathology, Av. Prof. Dr. Orlando Marques de Paiva 87, Cidade Universitária, 05508-270. São Paulo, Brazil. Tel: +55 11 30 91 12 00; Fax: +55 11 30 91 78 29. bcogliati@usp.br.
[†]These authors share equal seniorship.

Declaration of interest
The authors report no declarations of interest.

Europe PMC Funders Author Manuscripts

Keywords

connexin32; liver; fibrosis; apoptosis; oxidative stress

Europe PMC Funders Author Manuscripts

1 Introduction

Fibrosis is a wound healing response to various types of injury, whereby quiescent stellate cells transform into proliferative, fibrogenic and contractile myofibroblast-like cells. This is associated with a cascade of biochemical events, including chemotaxis, retinoid loss, pro-inflammatory cytokine release and collagen deposition (Friedman 2008). Liver fibrosis can progress into liver cirrhosis, which may further burgeon into hepatocellular carcinoma. In 2010, approximately 4% the worldwide deaths were due to liver cirrhosis (Lozano et al. 2012). Although this number varies depending on the region, it has been estimated that 0.1% and 1% of the European and North American population are affected by liver cirrhosis (Beste et al. 2015; Blachier et al. 2013). Besides the epidemiological relevance, liver fibrosis and cirrhosis also impose a considerable economic burden on society. Indeed, when conventional treatment fails, the only curative therapy for decompensated cirrhosis is liver transplantation (van Agthoven et al. 2001). However, liver transplantation is not a common practice, mainly because of lack of donor organs. It also has the disadvantage of requiring lifelong immunosuppression (Pillai and Levitsky 2009). Thus, it is clear that there is an urgent need for new therapies for the treatment of liver fibrosis.

Liver fibrosis is driven by a plethora of intracellular signaling cascades (Friedman 2008). The involvement of intercellular communication in this disease has been much less documented. Direct intercellular communication is mediated by gap junctions. Gap junctions are formed by the interaction of 2 hemichannels of neighbouring cells, which in their turn are built up by 6 connexin (Cx) proteins (Maes et al. 2014; Vinken et al. 2008). More than 20 different connexins have been identified in humans and rodents, all which are expressed in a cell-specific way (Kar et al. 2012). In liver, hepatocytes abundantly produce Cx32 next to small quantities of Cx26 (Nicholson et al. 1987), while non-parenchymal cells mainly harbour Cx43 (Fischer et al. 2005; González et al. 2002; Maes et al. 2014). Upon liver disease, however, Cx32 production is progressively downregulated typically at the expense of Cx43 (Maes et al. 2015). In this respect, decreased Cx32 protein amounts have been detected in liver tissue from patients with chronic liver disease (Maes et al. 2015; Nakashima et al. 2004; Yamaoka et al. 1995). This gradual disappearance of Cx32 has been experimentally reproduced on many occasions in rodents treated with the prototypical liver fibrotic agent carbon tetrachloride (CCl_4) (Cowles et al. 2007; Miyashita et al. 1991; Nakata et al. 1996). Nevertheless, the functional relevance of this deteriorative process and the role of Cx32 in liver fibrogenesis remain elusive.

In the present study, both wild-type (WT) and whole body Cx32 knock-out (KO) mice are treated with CCl_4 for extended periods of time. The resulting liver fibrotic response is evaluated based upon a series of clinically and/or mechanistically relevant parameters. By doing so, this work is anticipated to shed more light onto the role of Cx32 in chronic liver disease.

2 Methods

2.1 Animals and treatment

WT (Jackson Laboratories, USA) and $Cx32^{-/-}$ female mice with CD1 background were used in this study. $Cx32^{-/-}$ mice were kindly provided by Dr. Klaus Willecke (Nelles et al. 1996). Cx32 KO mice were generated by disrupting the Cx32 coding region in the mouse genome through insertion of a selectable gene that codes for neomycin resistance *via* homologous recombination (Evert et al. 2002; Nelles et al. 1996). Genotyping was performed by polymerase chain reaction (PCR) analysis of deoxyribonucleic acid (DNA) from mice tail-tips as previously described (Evert et al. 2002). Primers used for detection of the Cx32 WT allele were 5´-CCATAAGTCAGGTGTAAAGGAGC-3´ and 5´-AGATAAGCTGCAGGGACCATAGG-3´, generating a PCR product of 550 base pairs. Primer pairs used for detection of the Cx32-defective allele were 5´-CCATAAGTCAGGTGTAAAGGAGC-3´ and 5´-ATCATGCGAAACGATCCTCATCC-3´, generating a PCR product of 414 base pairs. Mice were housed under controlled conditions (*i.e.* 22-24°C, 65 ± 15% relative humidity, 12-hours light/dark cycle). 8-week-old mice of each genotype (n=10 *per* genotype) were weighed (22 ± 4 g) and received 3 weekly doses of 10% CCl_4 (Anidrol, Brazil) diluted in corn oil, intraperitoneally (ip), for 8 weeks. The initial dose of CCl_4 was 0.25 mg/kg, and there were 0.25 mg weekly increments to the utmost dose of 1.25 mg/kg (Cogliati et al. 2011). As control group of both genotypes, the animals received only the corn oil, ip (oil mice). All mice were weighed and sacrificed after 8 weeks of CCl_4 or oil treatment. The liver of each animal was weighed and relative liver weight was calculated. Blood samples were centrifuged for 10 minutes at 1503x*g* followed by harvesting of serum and storage at -20ºC. Fragments from each liver lobe were fixed in methacarn (*i.e.* 60% methanol, 30% chloroform and 10% acid acetic) for 12 hours and embedded in paraffin. Other liver fragments were snap-frozen in liquid nitrogen and stored at -80ºC. This study has been approved by the Committee on Bioethics of the School of Veterinary Medicine and Animal Science of the University of São Paulo (*i.e.* protocol number 811/2005) and all animals received human care according to the criteria outlined in the “Guide for the Care and Use of Laboratory Animals”.

2.2 Examination of liver histopathology and collagen morphometry

Paraffin-embedded liver fragments were cut and 5-μm tissue slides were stained with hematoxylin-eosin and Sirius Red. Histopathological evaluation of necro-inflammatory areas and fibrosis staging was performed as described elsewhere (Ishak et al. 1995). Quantification of collagen in liver histological sections stained with Sirius Red was carried as previously described (Cogliati et al. 2010). Briefly, the area corresponding to red collagen fibers was studied with a 20x objective microscope (Nikon, Japan) and quantified with appropriate computer software (Image ProPlus 4.5, Media Cybernetics, USA). The area of collagen fibers was expressed as percentage of the total area of liver tissue analyzed in 10 different random fields for each mouse. For the immunofluorescent staining of type-I collagen, histological sections were subjected to enzymatic digestion with 0.4% pepsin (Sigma, USA) diluted in 0.5 N acetic acid for 30 minutes at 37°C. Thereafter, sections were subsequently rinsed and incubated overnight in a moisturized chamber at 4°C with primary antibody (dilution 1:50) raised against type-I collagen (Rockland, USA). Next, slides were incubated

with secondary antibody swine anti-rabbit IgG, FITC-conjugated (dilution 1:100) (Dako, USA,). After 90 minutes incubation in a moist and dark chamber, sections were counterstained with propidium iodide (dilution 1:1000). Finally, slides were mounted with Vectashield (Vector Laboratories, USA), sealed with nail polish and photographed using a Nikon E-800 fluorescence microscope (Nikon, Japan) at magnification 20x.

2.3 Serum biochemistry

Alanine aminotransferase (ALT), aspartate aminotransferase (AST), alkaline phosphatase (ALP), bilirubin, total protein and albumin were measured with an automated bench-top dry chemistry analyzer (IDEXX Laboratories Ltd, UK). ALT, AST and ALP values were expressed in U/L, bilirubin was expressed in mg/dL and total protein and albumin were expressed in g/dL.

2.4 Hepatic protein extraction and quantification

Frozen liver tissue weighing approximately 30 mg was homogenized in lysis buffer with protease inhibitors (Roche, Germany). Homogenates were centrifuged at 14000*xg* for 10 minutes at 4°C and protein concentrations in supernatants were determined according to the Bradford procedure (Bradford 1976) using a commercial kit (Bio-Rad, USA) with bovine serum albumin as a standard.

2.5 Analysis of hepatic anti-oxidant enzymes

The superoxide dismutase (SOD) activity was assayed according to Ewin and Janero (Ewing and Janero 1995). SOD activity from the liver homogenate (*i.e.* 25 μL) was monitored at 560 nm over 5 minutes at 26ºC by detecting formazan generation. A standard curve was prepared with a range between 0.69 U/mg protein and 22.15 U/mg protein of SOD from bovine erythrocytes (Sigma, USA). Glutathione peroxidase (GPx) activity was determined as previously described (Flohé and Günzler 1984). GPx activity from liver homogenate containing 2 mg/mL of protein (*i.e.* 30 μL) was continuously monitored at 340 nm absorbance over 4 minutes at 37°C by the detection of nicotinamide adenine dinucleotide phosphate. The standard curve was prepared with GPx from 1.5 U/mg protein to 50 U/mg protein (Sigma, USA). Glutathione reductase activity was determined as previously described by Torres and group (Torres et al. 2011). GR activity was continuously monitored in 20 μL from the liver homogenate containing 4 mg/mL of protein at absorbance of 340 nm over 26 minutes at 37°C by the measurement of nicotinamide adenine dinucleotide phosphate oxidation. The standard curve was prepared with GR from 0.0003 U/mL to 0.25 U/mL of protein (Sigma, USA). The catalase activity was determined according to Bonaventura et al. (Bonaventura et al. 1972). Catalase activity was continuously monitored in liver homogenate containing 0.05 μg/μL of protein (*i.e.* 20 μL) at a 240 nm absorbance over 8 minutes at 30°C by the measurement of hydrogen peroxide (H_2O_2). A standard curve was prepared using catalase enzyme (Sigma, USA) and enzymatic activity was expressed in U/mg protein.

Europe PMC Funders Author Manuscripts

2.6 Analysis of liver malondialdehyde

Malondialdehyde (MDA) levels in protein extracts were determined by reverse phase high-performance liquid chromatography (HPLC) according to the protocol introduced by Hong and co-workers (Hong et al. 2000). Thiobarbituric acid-MDA conjugate derivative was injected into a Phenomenex reverse-phase C18 analytical column (250 mm x 4.6 mm, 5 mm Phenomenex, USA) with a LC8-D8 pre-column (Phenomenex, USA) and was fluorometrically quantified at an excitation wave length of 515 nm and an emission wave length of 553 nm. The HPLC pump delivered the isocratic mobile phase at a flow rate of 1.0 mL *per* minute. A standard curve was prepared using 1,1,3,3-tetraetoxipropano. The results were expressed in μM/mg protein.

2.7 Enzyme-linked immunosorbent assay assays for liver inflammatory cytokines and cleaved caspase 3

Enzyme-linked immunosorbent assay (ELISA) kits were used to measure levels of mouse interleukin (IL)-1β, IL-6, IL-10, interferon γ (IFNγ) and tumor necrosis factor α (TNFα) (BD Biosciences, USA), and cleaved caspase 3 (RD systems, USA). Wells of a 96-well plate were coated overnight with appropriate monoclonal antibody diluted in coating buffer and blocked for 1 hour for the inflammatory cytokines and 1.5 hours for cleaved caspase 3 with phosphate-buffered saline containing bovine serum albumin. Subsequently, wells were incubated with liver homogenate or standard solution for 2 hours followed by incubation with appropriate biotinylated monoclonal antibody and streptavidin-horseradish peroxidase conjugate for 1 hour and 30 minutes, respectively. For caspase 3 analysis, the incubation times were 2 hours and 20 minutes. Finally, wells were exposed to tetramethylbenzidine substrate reagent for 30 minutes. The reaction was stopped by adding phosphoric acid for the cytokine measurements and sulfuric acid for caspase 3 analyses. The absorbance was measured at 450 nm with wavelength correction at 570 nm using a Varioskan™ Flash Multimode Reader (Thermo Scientific, USA). Values were expressed as pg/mg of protein.

2.8 Immunoblot analysis of pro/anti-apoptotic proteins and proliferating cell nuclear antigen

Sixty μg of protein from the samples were resolved on 12% Mini-Protean^{R} TGX™ gel (Bio-Rad, USA) and transferred with the iBlot system to Novex (Invitrogen, USA). Membranes were blocked with 5% non-fatty milk in Tris-buffered saline solution (*i.e.* 20 mM Tris and 135 mM sodium chloride) containing 0.1% Tween-20 (Bio-Rad, USA) during 1 hour. Membranes were probed overnight at 4ºC with primary antibodies directed against mouse Bid, Bax, and Bcl-xL (Cell Signaling Technology, USA) at 1:1000 dilution and against proliferating cell nuclear antigen (Sewnath et al.) (Santa Cruz, USA) at 1:200 dilution. Following incubation for 1 hour with horseradish peroxidase-labeled secondary antibody (Dako, USA), membranes were processed with the Pierce™ enhanced chemiluminescence Western blotting substrate kit (Thermo Scientific, USA) according to the manufacturer's instructions and signals were visualized with the ChemiDoc™ MP Imaging system (Bio-Rad, USA). Densitometric analyses were performed using Image Lab 5.2 (Bio-Rad, USA). For semi-quantification purposes, Bid, Bax, Bcl-xL and PCNA signals were normalized against β-actin signals and expressed as relative alterations compared to WT animals.

2.9 Quantitative real-time PCR analysis

The quantitative PCR technique was performed following the Minimum Information for Publication of Quantitative Real-Time PCR Experiments guidelines (Bustin et al. 2009). Total ribonucleic acid (RNA) (i.e. 3 μg) was isolated from liver tissue using the RNAspin mini RNA isolation kit (GE HealthCare, USA) and was reverse transcribed to copy DNA using random primers and VILO Master Mix kit (Invitrogen). Collagen α1(I) primers and probes (assay ID Mm00801666_g1) for real-time PCR were purchased from Applied Biosystems (USA). 18S rRNA (assay ID Mm04277571_s1) and ACTB (assay ID Mm00607939_s1) were used as reference genes to normalize the results. Each sample was analyzed in duplicate and negative controls were enrolled. Efficiency was verified and established between 95% and 105%. Analyses were carried out using an ABI PRISM 7000 device (Applied Biosystems, USA). Analyses of relative gene expression data were performed according to the $2^{-\Delta\Delta Cq}$ method (Livak and Schmittgen, 2001). Results were expressed as fold change of ΔΔCq values obtained from WT oil mice.

2.10 Statistical analysis

The number of repeats (n) for each analysis varied and is specified in the discussion of the results. All data were expressed as mean ± standard error of the mean. Comparison of parameters between different genotypes or groups was performed using unpaired student *t*-tests with 2-tailed comparisons using GraphPad Prism6 software. Probability (p) values of less than or equal to 0.05 were considered as significant.

3 Results

3.1 Cx32 deficiency enhances liver fibrosis after CCl_4-induced chronic hepatic injury

Hepatic biotransformation of CCl_4 relies on cytochrome P450 2E1 and yields the trichloromethyl radical, which is involved in several reactions generating free radicals and lipid peroxidation (Basu 2003). This contributes to an acute phase reaction characterized by cell death of centrilobular hepatocytes, the activation of Kupffer cells and the induction of an inflammatory response. This is associated with the production of several cytokines, which promote activation of hepatic stellate cells (HSCs) and hence liver fibrosis (Iwaisako et al. 2014). Upon treatment of WT and $Cx32^{-/-}$ mice with CCl_4 for 8 weeks, both groups showed equal nodule formation and no difference in relative liver weight was observed. Both WT and $Cx32^{-/-}$ untreated mice (oil) did not present any liver alteration related to fibrosis deposition (Figure 1). The mortality rate was less than 5% in both fibrotic WT and $Cx32^{-/-}$ mice. Morphometric analysis following *in situ* staining of collagen with Sirius red showed a significant ($p < 0.001$) increase in the normalized collagen area ratio in liver tissue of fibrotic $Cx32^{-/-}$ mice compared to WT animals, which was confirmed by immunolabeling of type-I collagen and at the mRNA level of collagen α1(I) ($p < 0.01$) (Figure 1).

3.2 Cx32 deficiency enhances hepatocellular injury after CCl_4-induced chronic hepatic injury

Morphological alterations caused by CCl_4 were observed on liver sections stained by hematoxylin-eosin and evaluated according to the classification of Ishak and group (1995)

from both mice genotypes. Based upon on histopathological analysis, a significant ($p < 0.05$) increase in histological necro-inflammatory activity was found in fibrotic $Cx32^{-/-}$ mice compared to WT counterparts (Figure 2). These findings were reflected at the biochemical level, as CCl_4-treated $Cx32^{-/-}$ mice showed significantly elevated serum levels of AST ($p < 0.01$) and ALT ($p < 0.05$) (Table 1). Both cytosolic enzymes leak from the cell into the serum upon membrane damage, such as occurring in case of necrosis, and indicate liver malfunction (Adams 2011; Poupon 2015). No differences were observed in other serum parameters tested, including ALP, albumin, total protein and bilirubin (Table 1). Taken together, these results point to aggravation of CCl_4-related liver injury and, consequently, more pronounced collagen deposition upon genetic ablation of Cx32.

3.3 Cx32 deficiency does not increase inflammatory cytokines release after CCl_4-induced chronic hepatic injury

The biotransformation of CCl_4 leads to hepatocyte death and reactive oxygen species production, which concomitantly activate the inflammatory machinery in the liver and the release of both pro-inflammatory as well as anti-inflammatory cytokines (Gieling et al. 2009; Knittel et al. 1997; Luckey and Petersen 2001; Simeonova et al. 2001). Accordingly, a number of pro-inflammatory cytokines, namely IL1β, IL6, TNFα and IFNγ, and the anti-inflammatory cytokine IL10 were measured in liver samples. Apart from slightly increased hepatic levels of IL1β, IL6 and TNFα, and modestly decreased IL10 quantities in fibrotic $Cx32^{-/-}$ mice, no difference between both genotypes could be detected (Figure 2). Thus, lack of Cx32 does not affect the release of cytokines following CCl_4-induced liver fibrosis.

3.4 Cx32 deficiency decreases catalase activity and increases malondialdehyde in liver after CCl_4-induced chronic hepatic injury

Free radicals and lipid peroxidation underlie liver disease from a broad variety of etiologies (Muriel 2009). Lipid peroxidation is a process by which free radicals attack lipids containing carbon-carbon double bonds, especially polyunsaturated fatty acids. One of the main lipid peroxidation products related to CCl_4-induced chronic hepatic injury is MDA (Hartley et al. 1999), which triggers cytotoxicity (Ayala et al. 2014). There are several major classes of free radicals scavengers in the liver, including SOD, catalase, GR and GPx. In CCl_4-based animal models of hepatotoxicity, decreased anti-oxidant enzymatic activity has been observed (Szymonik-Lesiuk et al. 2003; Zhang et al. 2015), which favors liver damage as well as the progression of the fibrotic response. Therefore, a number of prominent anti-oxidant enzymes, including SOD, catalase, GR and GPx, were evaluated in this study together with the measurement of hepatic levels of MDA. No differences in their enzyme activity could be detected between cohorts, with the exception of catalase activity, which was significantly ($p < 0.05$) decreased in Cx32-deficient animals (Figure 3). By contrast, MDA quantities were significantly ($p < 0.05$) upregulated in $Cx32^{-/-}$ mice (Figure 3). Overall, these results indicate a more prominent oxidative stress response to CCl_4-induced chronic hepatic injury in the absence of Cx32, which is in line with the more pronounced liver damage and fibrosis response.

3.5 Cx32 deficiency does not alter apoptotic signaling or regenerative activity after CCl_4-induced chronic hepatic injury

Hepatocellular apoptosis after injury contributes to the initiation and perpetuation of the fibrotic response (Canbay et al. 2002; Lee et al. 2011). A key step in apoptotic signaling is the translocation of Bax and the truncated form of Bid into the mitochondria, which ultimately leads to the activation of caspase 3, being the main executor of cell death (Gross et al. 1999; Hikita et al. 2011). Other members of the Bcl-2 family, such as Bcl-xL, rather display anti-apoptotic activity (Gross et al. 1999). In the present study, protein expression analysis of Bid, Bax, cleaved caspase 3 and Bcl-xL showed no differences between WT and $Cx32^{-/-}$ mice (Figure 4). In addition to injury mechanisms, initiation of regeneration and thus proliferation are critical for repair of damaged liver tissue and recovery after CCl_4-induced liver injury (Louis et al. 1998). PCNA expression is commonly used as a read-out to monitor regenerative activity in liver following injury (de Gouville et al. 2005; Louis et al. 1998). Immunoblot analysis showed no statistical difference in PCNA protein amounts between fibrotic $Cx32^{-/-}$ and WT mice (Figure 4). In summary, these data suggest that Cx32 may not be involved in the regulation of the regenerative capacity nor in apoptotic signaling response to CCl_4-induced liver fibrosis.

4 Discussion

Given the important roles of gap junctions in liver functionality (Vinken et al. 2008) and hence in the maintenance of hepatic homeostasis, it is not surprising that they are frequently involved in liver toxicity and disease (Maes et al. 2015; Vinken et al. 2008). Cx32 dominant negative transgenic rats display reduced liver damage in comparison with WT counterparts when administered prototypical liver toxicants, such as *D*-galactosamine (Asamoto et al. 2004) or acetaminophen (Naiki-Ito et al. 2010). This suggests that Cx32-based signaling may intensify hepatic injury. By contrast, $Cx32^{-/-}$ mice are known to be much more prone to both chemically induced and spontaneously occurring liver cancer (Dagli et al. 2004; Temme et al. 1997). This rather points to a cytoprotective function of Cx32-based communication in liver. With respect to the role of connexins in liver fibrosis, our group previously reported that repeated administration of CCl_4 to Cx43-deficient mice results in excessive liver fibrosis compared with WT animals. These animals also presented less necro-inflammatory lesions on liver parenchyma, lower serum ALT and AST levels as well as diminished hepatocyte proliferation. These findings suggest that Cx43 fulfils a key function in hepatic fibrogenesis (Cogliati et al. 2011). In the present study, a similar approach was used to elucidate the role of Cx32 in liver fibrosis.

Our results indicate that lack of Cx32 induces a marked increase in the histopathological necro-inflammatory index as well as in serum levels of AST and ALT, which is accompanied by enhanced collagen deposition. These observations suggest that absence of Cx32 signaling may result in more pronounced liver damage. The lack of difference in ALP levels confirmed the absence of injury in the bile ducts, which express Cx43 (Bode et al. 2002). We further investigated the possible involvement of Cx32 in apoptotic signaling during chronic fibrotic liver injury. This programmed cell death mechanism is a major driver of the fibrotic response, facilitating both HSC activation and inflammation (Lee et al. 2011). In this

respect, Bax and caspase 3 have been reported to be upregulated in CCl_4-induced liver fibrosis in rat (Liang et al. 2015). Moreover, deficiency of anti-apoptotic Bcl-xL results in sustained hepatocyte apoptosis and concomitantly promotes the development of fibrosis (Takehara et al. 2004). Despite the documented importance of this cell death mode in the perpetuation of fibrosis, our results show that the absence of Cx32 has no effect on the protein levels of Bid, Bax, caspase 3 and Bcl-xL. This is in line with previously published studies in animal models of acute pancreatitis and in acetaminophen-induced acute liver failure, in which the apoptotic signaling remained unchanged in negative Cx32 mutants (Frossard et al. 2003; Igarashi et al. 2014). Alternatively, oxidative stress may induce HSC activation (Nieto et al. 2002a, b). In our study, oxidative stress result from decreased catalase activity in Cx32 deficient mice, which maintained high levels of the H_2O_2 generated from the biotransformation of CCl_4 by cytochrome P450 2E1 in hepatocytes. As a consequence, the production of oxygen reactive species and thus MDA becomes increased, which in turn can trigger cytotoxicity (Ayala et al. 2014). This could explain the elevated levels of liver injury and enhanced collagen deposition observed in Cx32-depleted mice. Although no association between catalase and Cx32 has been reported thus far, Fukuda and coworkers observed that the preservation of Cx32 production by taurine contributed to the anti-oxidant effect in the presence of H_2O_2 (Fukuda et al. 2000). This anti-oxidant effect also became manifested upon exposure of primary hepatocytes to dimethyl sulfoxide, dimethylthiourea and melatonin (Kojima et al. 1996; Kojima et al. 1997). Gap junctions have been described to play a critical role in liver-specific functionality, liver development, hepatocyte growth and cell death (Vinken 2012). It has been suggested that the disappearance of these structures during disease disrupts tissue homeostasis, by allowing intracellular peroxide levels to augment, subsequently leading to inhibition of catalase activity (Lardinois et al. 1996). These findings suggest that Cx32 may play a role in the maintenance of the cellular anti-oxidant activity to counteract cell damage and liver fibrosis.

The inflammatory response associated with cell death and oxidative stress (Rock and Kono 2008) can alter the expression and activity of liver gap junctions (De Maio et al. 2000; Gingalewski et al. 1996). Inflammatory cytokines, such as IL1β, TNFα and IL6 have been repeatedly found to negatively affect hepatic Cx32 production (Brosnan et al. 2001; González et al. 2002). Indeed, these cytokines modify the stability of Cx32mRNA (Gingalewski et al. 1996; Theodorakis and De Maio 1999). In the present study, we could not observe significant differences in pro-inflammatory and anti-inflammatory cytokine amounts between WT and $Cx32^{-/-}$ mice, which could indicate that Cx32 is not required for cytokine release. We next tested the hypothesis that Cx32 signaling may counteract liver fibrosis by affecting the regenerative capacity. For this purpose, we measured protein quantities of PCNA, yet no difference could be detected between cohorts. This is consistent with the observations made by Yamamoto and coworkers (Yamamoto et al. 2005), showing that the absence or presence of Cx32 in livers after partial hepatectomy does not affect regenerative capacity (Yamamoto et al. 2005). In accordance with these results, Cx32 did not modulate liver regeneration in fibrosis.

Europe PMC Funders Author Manuscripts

5 Conclusion

The present study has pointed the role of Cx32 in tissue protection during liver fibrosis. It was found that the ablation of Cx32, although lack of involvement in the evaluated markers of apoptosis, oxidative stress, inflammatory or regeneration; it may modulates the catalase activity and thus influence MDA levels in the liver. Consequently, this supports the possible role of Cx32 in tissue protection against chronic liver injury by the modulation of the anti-oxidant cellular capacity. This potentially has clinical implications, as enhancement of Cx32 production may represent a therapeutic strategy to counteract hepatocyte damage and, consequently, liver fibrosis.

Acknowledgements

This work was financially supported by the grants of the 'Fundação de Auxílio à Pesquisa do Estado de São Paulo' (FAPESP grants 06/56138-7; 05/59583-9 and SPEC 13/50420-6), the European Research Council (ERC Starting Grant 335476), the Fund for Scientific Research-Flanders (FWO grants G009514N and G010214N) and the University Hospital of the Vrije Universiteit Brussel-Belgium (“Willy Gepts Fonds” UZ-VUB).

List of abbreviations

ALP	alkaline phosphatase
ALT	alanine amintransferase
AST	aspartate aminotransferase
CCl_4	carbon tetrachloride
DNA	deoxyribonucleic acid
Cx	connexin
ELISA	enzyme-linked immunosorbent assay
GPx	glutathione peroxidase
GR	glutathione reductase
HPLC	high-performance liquid chromatography
HSCs	hepatic stellate cells
H_2O_2	hydrogen peroxide
IFNγ	interferon γ
IL	interleukin
ip	intraperitoneal
KO	knock-out
MDA	malondialdehyde

n	number of repeats
p	probability
PCNA	proliferating cell nuclear antigen
PCR	polymerase chain reaction
RNA	ribonucleic acid
SEM	standard error of the mean
SOD	superoxide dismutase
TNFα	tumor necrosis factor α
WT	wild-type

References

Adams LA. Biomarkers of liver fibrosis. J Gastroenterol Hepatol. 2011; 26:802–809. [PubMed: 21198831]

Asamoto M, Hokaiwado N, Murasaki T, Shirai T. Connexin 32 dominant-negative mutant transgenic rats are resistant to hepatic damage by chemicals. Hepatology. 2004; 40:205–210. [PubMed: 15239104]

Ayala A, Muñoz MF, Argüelles S. Lipid peroxidation: production, metabolism, and signaling mechanisms of malondialdehyde and 4-hydroxy-2-nonenal. Oxid Med Cell Longev. 2014; 2014:360438. [PubMed: 24999379]

Basu S. Carbon tetrachloride-induced lipid peroxidation: eicosanoid formation and their regulation by antioxidant nutrients. Toxicology. 2003; 189:113–127. [PubMed: 12821287]

Beste LA, Leipertz SL, Green PK, Dominitz JA, Ross D, Ioannou GN. Trends in Burden of Cirrhosis and Hepatocellular Carcinoma by Underlying Liver Disease in US Veterans, 2001-2013. Gastroenterology. 2015; 149:1471–1482.e1475. [PubMed: 26255044]

Blachier M, Leleu H, Peck-Radosavljevic M, Valla DC, Roudot-Thoraval F. The burden of liver disease in Europe: a review of available epidemiological data. J Hepatol. 2013; 58:593–608. [PubMed: 23419824]

Bode HP, Wang L, Cassio D, Leite MF, St-Pierre MV, Hirata K, Okazaki K, Sears ML, Meda P, Nathanson MH, Dufour JF. Expression and regulation of gap junctions in rat cholangiocytes. Hepatology. 2002; 36:631–640. [PubMed: 12198655]

Bonaventura J, Schroeder WA, Fang S. Human erythrocyte catalase: an improved method of isolation and a reevaluation of reported properties. Arch Biochem Biophys. 1972; 150:606–617. [PubMed: 5044042]

Bradford MM. A rapid and sensitive method for the quantitation of microgram quantities of protein utilizing the principle of protein-dye binding. Anal Biochem. 1976; 72:248–254. [PubMed: 942051]

Brosnan CF, Scemes E, Spray DC. Cytokine regulation of gap junction connectivity: an open-and-shut case or changing partners at the Nexus? Am J Pathol. 2001; 158:1565–1569. [PubMed: 11337352]

Bustin SA, Benes V, Garson JA, Hellemans J, Huggett J, Kubista M, Mueller R, Nolan T, Pfaffl MW, Shipley GL, Vandesompele J, et al. The MIQE guidelines: minimum information for publication of quantitative real-time PCR experiments. Clin Chem. 2009; 55:611–622. [PubMed: 19246619]

Canbay A, Higuchi H, Bronk SF, Taniai M, Sebo TJ, Gores GJ. Fas enhances fibrogenesis in the bile duct ligated mouse: a link between apoptosis and fibrosis. Gastroenterology. 2002; 123:1323–1330. [PubMed: 12360492]

Cogliati B, Da Silva TC, Aloia TP, Chaible LM, Real-Lima MA, Sanches DS, Matsuzaki P, Hernandez-Blazquez FJ, Dagli ML. Morphological and molecular pathology of CCL4-induced

hepatic fibrosis in connexin43-deficient mice. Microsc Res Tech. 2011; 74:421–429. [PubMed: 20830702]

Cogliati B, Pereira HeM, Dagli ML, Parra OM, Silva JR, Hernandez-Blazquez FJ. Hepatotrophic factors reduce hepatic fibrosis in rats. Arq Gastroenterol. 2010; 47:79–85. [PubMed: 20520980]

Cowles C, Mally A, Chipman JK. Different mechanisms of modulation of gap junction communication by non-genotoxic carcinogens in rat liver in vivo. Toxicology. 2007; 238:49–59. [PubMed: 17624652]

Dagli ML, Yamasaki H, Krutovskikh V, Omori Y. Delayed liver regeneration and increased susceptibility to chemical hepatocarcinogenesis in transgenic mice expressing a dominant-negative mutant of connexin32 only in the liver. Carcinogenesis. 2004; 25:483–492. [PubMed: 14688024]

de Gouville AC, Boullay V, Krysa G, Pilot J, Brusq JM, Loriolle F, Gauthier JM, Papworth SA, Laroze A, Gellibert F, Huet S. Inhibition of TGF-beta signaling by an ALK5 inhibitor protects rats from dimethylnitrosamine-induced liver fibrosis. Br J Pharmacol. 2005; 145:166–177. [PubMed: 15723089]

De Maio A, Gingalewski C, Theodorakis NG, Clemens MG. Interruption of hepatic gap junctional communication in the rat during inflammation induced by bacterial lipopolysaccharide. Shock. 2000; 14:53–59. [PubMed: 10909894]

Evert M, Ott T, Temme A, Willecke K, Dombrowski F. Morphology and morphometric investigation of hepatocellular preneoplastic lesions and neoplasms in connexin32-deficient mice. Carcinogenesis. 2002; 23:697–703. [PubMed: 12016140]

Ewing JF, Janero DR. Microplate superoxide dismutase assay employing a nonenzymatic superoxide generator. Anal Biochem. 1995; 232:243–248. [PubMed: 8747482]

Fischer R, Reinehr R, Lu TP, Schönicke A, Warskulat U, Dienes HP, Häussinger D. Intercellular communication via gap junctions in activated rat hepatic stellate cells. Gastroenterology. 2005; 128:433–448. [PubMed: 15685554]

Flohé L, Günzler WA. Assays of glutathione peroxidase. Methods Enzymol. 1984; 105:114–121. [PubMed: 6727659]

Friedman SL. Mechanisms of hepatic fibrogenesis. Gastroenterology. 2008; 134:1655–1669. [PubMed: 18471545]

Frossard JL, Rubbia-Brandt L, Wallig MA, Benathan M, Ott T, Morel P, Hadengue A, Suter S, Willecke K, Chanson M. Severe acute pancreatitis and reduced acinar cell apoptosis in the exocrine pancreas of mice deficient for the Cx32 gene. Gastroenterology. 2003; 124:481–493. [PubMed: 12557153]

Fukuda T, Ikejima K, Hirose M, Takei Y, Watanabe S, Sato N. Taurine preserves gap junctional intercellular communication in rat hepatocytes under oxidative stress. J Gastroenterol. 2000; 35:361–368. [PubMed: 10832671]

Gieling RG, Wallace K, Han YP. Interleukin-1 participates in the progression from liver injury to fibrosis. Am J Physiol Gastrointest Liver Physiol. 2009; 296:G1324–1331. [PubMed: 19342509]

Gingalewski C, Wang K, Clemens MG, De Maio A. Posttranscriptional regulation of connexin 32 expression in liver during acute inflammation. J Cell Physiol. 1996; 166:461–467. [PubMed: 8592007]

González HE, Eugenín EA, Garcés G, Solís N, Pizarro M, Accatino L, Sáez JC. Regulation of hepatic connexins in cholestasis: possible involvement of Kupffer cells and inflammatory mediators. Am J Physiol Gastrointest Liver Physiol. 2002; 282:G991–G1001. [PubMed: 12016124]

Gross A, Yin XM, Wang K, Wei MC, Jockel J, Milliman C, Erdjument-Bromage H, Tempst P, Korsmeyer SJ. Caspase cleaved BID targets mitochondria and is required for cytochrome c release, while BCL-XL prevents this release but not tumor necrosis factor-R1/Fas death. J Biol Chem. 1999; 274:1156–1163. [PubMed: 9873064]

Hartley DP, Kolaja KL, Reichard J, Petersen DR. 4-Hydroxynonenal and malondialdehyde hepatic protein adducts in rats treated with carbon tetrachloride: immunochemical detection and lobular localization. Toxicol Appl Pharmacol. 1999; 161:23–33. [PubMed: 10558920]

Hikita H, Takehara T, Kodama T, Shimizu S, Shigekawa M, Hosui A, Miyagi T, Tatsumi T, Ishida H, Li W, Kanto T, et al. Delayed-onset caspase-dependent massive hepatocyte apoptosis upon Fas activation in Bak/Bax-deficient mice. Hepatology. 2011; 54:240–251. [PubMed: 21425311]

Hong YL, Yeh SL, Chang CY, Hu ML. Total plasma malondialdehyde levels in 16 Taiwanese college students determined by various thiobarbituric acid tests and an improved high-performance liquid chromatography-based method. Clin Biochem. 2000; 33:619–625. [PubMed: 11166008]

Igarashi I, Maejima T, Kai K, Arakawa S, Teranishi M, Sanbuissho A. Role of connexin 32 in acetaminophen toxicity in a knockout mice model. Exp Toxicol Pathol. 2014; 66:103–110. [PubMed: 24263089]

Ishak K, Baptista A, Bianchi L, Callea F, De Groote J, Gudat F, Denk H, Desmet V, Korb G, MacSween RN. Histological grading and staging of chronic hepatitis. J Hepatol. 1995; 22:696–699. [PubMed: 7560864]

Iwaisako K, Jiang C, Zhang M, Cong M, Moore-Morris TJ, Park TJ, Liu X, Xu J, Wang P, Paik YH, Meng F, et al. Origin of myofibroblasts in the fibrotic liver in mice. Proc Natl Acad Sci U S A. 2014; 111:E3297–3305. [PubMed: 25074909]

Kar R, Batra N, Riquelme MA, Jiang JX. Biological role of connexin intercellular channels and hemichannels. Arch Biochem Biophys. 2012; 524:2–15. [PubMed: 22430362]

Knittel T, Müller L, Saile B, Ramadori G. Effect of tumour necrosis factor-alpha on proliferation, activation and protein synthesis of rat hepatic stellate cells. J Hepatol. 1997; 27:1067–1080. [PubMed: 9453433]

Kojima T, Mitaka T, Mizuguchi T, Mochizuki Y. Effects of oxygen radical scavengers on connexins 32 and 26 expression in primary cultures of adult rat hepatocytes. Carcinogenesis. 1996; 17:537–544. [PubMed: 8631141]

Kojima T, Mochizuki C, Mitaka T, Mochizuki Y. Effects of melatonin on proliferation, oxidative stress and Cx32 gap junction protein expression in primary cultures of adult rat hepatocytes. Cell Struct Funct. 1997; 22:347–356. [PubMed: 9248998]

Lardinois OM, Mestdagh MM, Rouxhet PG. Reversible inhibition and irreversible inactivation of catalase in presence of hydrogen peroxide. Biochim Biophys Acta. 1996; 1295:222–238. [PubMed: 8695649]

Lee TF, Lin YL, Huang YT. Kaerophyllin inhibits hepatic stellate cell activation by apoptotic bodies from hepatocytes. Liver Int. 2011; 31:618–629. [PubMed: 21457435]

Liang B, Guo XL, Jin J, Ma YC, Feng ZQ. Glycyrrhizic acid inhibits apoptosis and fibrosis in carbon-tetrachloride-induced rat liver injury. World J Gastroenterol. 2015; 21:5271–5280. [PubMed: 25954100]

Livak KJ, Schmittgen TD. Analysis of relative gene expression data using real-time quantitative PCR and the 2(-Delta Delta C(T)) method. Methods. 2001; 25:402–408. [PubMed: 11846609]

Louis H, Van Laethem JL, Wu W, Quertinmont E, Degraef C, Van den Berg K, Demols A, Goldman M, Le Moine O, Geerts A, Devière J. Interleukin-10 controls neutrophilic infiltration, hepatocyte proliferation, and liver fibrosis induced by carbon tetrachloride in mice. Hepatology. 1998; 28:1607–1615. [PubMed: 9828225]

Lozano R, Naghavi M, Foreman K, Lim S, Shibuya K, Aboyans V, Abraham J, Adair T, Aggarwal R, Ahn SY, Alvarado M, et al. Global and regional mortality from 235 causes of death for 20 age groups in 1990 and 2010: a systematic analysis for the Global Burden of Disease Study 2010. Lancet. 2012; 380:2095–2128. [PubMed: 23245604]

Luckey SW, Petersen DR. Activation of Kupffer cells during the course of carbon tetrachloride-induced liver injury and fibrosis in rats. Exp Mol Pathol. 2001; 71:226–240. [PubMed: 11733948]

Maes M, Crespo Yanguas S, Willebrords J, Cogliati B, Vinken M. Connexin and pannexin signaling in gastrointestinal and liver disease. Transl Res. 2015; 166:332–343. [PubMed: 26051630]

Maes M, Decrock E, Cogliati B, Oliveira AG, Marques PE, Dagli ML, Menezes GB, Mennecier G, Leybaert L, Vanhaecke T, Rogiers V, et al. Connexin and pannexin (hemi)channels in the liver. Front Physiol. 2014; 4:405. [PubMed: 24454290]

Miyashita T, Takeda A, Iwai M, Shimazu T. Single administration of hepatotoxic chemicals transiently decreases the gap-junction-protein levels of connexin 32 in rat liver. Eur J Biochem. 1991; 196:37–42. [PubMed: 1848185]

Muriel P. Role of free radicals in liver diseases. Hepatol Int. 2009; 3:526–536. [PubMed: 19941170]

Naiki-Ito A, Asamoto M, Naiki T, Ogawa K, Takahashi S, Sato S, Shirai T. Gap junction dysfunction reduces acetaminophen hepatotoxicity with impact on apoptotic signaling and connexin 43 protein induction in rat. Toxicol Pathol. 2010; 38:280–286. [PubMed: 20097795]

Nakashima Y, Ono T, Yamanoi A, El-Assal ON, Kohno H, Nagasue N. Expression of gap junction protein connexin32 in chronic hepatitis, liver cirrhosis, and hepatocellular carcinoma. J Gastroenterol. 2004; 39:763–768. [PubMed: 15338370]

Nakata Y, Iwai M, Kimura S, Shimazu T. Prolonged decrease in hepatic connexin32 in chronic liver injury induced by carbon tetrachloride in rats. J Hepatol. 1996; 25:529–537. [PubMed: 8912153]

Nelles E, Bützler C, Jung D, Temme A, Gabriel HD, Dahl U, Traub O, Stümpel F, Jungermann K, Zielasek J, Toyka KV, et al. Defective propagation of signals generated by sympathetic nerve stimulation in the liver of connexin32-deficient mice. Proc Natl Acad Sci U S A. 1996; 93:9565–9570. [PubMed: 8790370]

Nicholson B, Dermietzel R, Teplow D, Traub O, Willecke K, Revel JP. Two homologous protein components of hepatic gap junctions. Nature. 1987; 329:732–734. [PubMed: 2823143]

Nieto N, Friedman SL, Cederbaum AI. Cytochrome P450 2E1-derived reactive oxygen species mediate paracrine stimulation of collagen I protein synthesis by hepatic stellate cells. J Biol Chem. 2002a; 277:9853–9864. [PubMed: 11782477]

Nieto N, Friedman SL, Cederbaum AI. Stimulation and proliferation of primary rat hepatic stellate cells by cytochrome P450 2E1-derived reactive oxygen species. Hepatology. 2002b; 35:62–73. [PubMed: 11786960]

Pillai AA, Levitsky J. Overview of immunosuppression in liver transplantation. World J Gastroenterol. 2009; 15:4225–4233. [PubMed: 19750565]

Poupon R. Liver alkaline phosphatase: a missing link between choleresis and biliary inflammation. Hepatology. 2015; 61:2080–2090. [PubMed: 25603770]

Rock KL, Kono H. The inflammatory response to cell death. Annu Rev Pathol. 2008; 3:99–126. [PubMed: 18039143]

Sewnath ME, Van Der Poll T, Van Noorden CJ, Ten Kate FJ, Gouma DJ. Endogenous interferon gamma protects against cholestatic liver injury in mice. Hepatology. 2002; 36:1466–1477. [PubMed: 12447873]

Simeonova PP, Gallucci RM, Hulderman T, Wilson R, Kommineni C, Rao M, Luster MI. The role of tumor necrosis factor-alpha in liver toxicity, inflammation, and fibrosis induced by carbon tetrachloride. Toxicol Appl Pharmacol. 2001; 177:112–120. [PubMed: 11740910]

Szymonik-Lesiuk S, Czechowska G, Stryjecka-Zimmer M, Słomka M, Madro A, Celiński K, Wielosz M. Catalase, superoxide dismutase, and glutathione peroxidase activities in various rat tissues after carbon tetrachloride intoxication. J Hepatobiliary Pancreat Surg. 2003; 10:309–315. [PubMed: 14598152]

Takehara T, Tatsumi T, Suzuki T, Rucker EB, Hennighausen L, Jinushi M, Miyagi T, Kanazawa Y, Hayashi N. Hepatocyte-specific disruption of Bcl-xL leads to continuous hepatocyte apoptosis and liver fibrotic responses. Gastroenterology. 2004; 127:1189–1197. [PubMed: 15480996]

Temme A, Buchmann A, Gabriel HD, Nelles E, Schwarz M, Willecke K. High incidence of spontaneous and chemically induced liver tumors in mice deficient for connexin32. Curr Biol. 1997; 7:713–716. [PubMed: 9285723]

Theodorakis NG, De Maio A. Cx32 mRNA in rat liver: effects of inflammation on poly(A) tail distribution and mRNA degradation. Am J Physiol. 1999; 276:R1249–1257. [PubMed: 10233014]

Torres LL, Quaglio NB, de Souza GT, Garcia RT, Dati LM, Moreira WL, Loureiro AP, de Souza-Talarico JN, Smid J, Porto CS, Bottino CM, et al. Peripheral oxidative stress biomarkers in mild cognitive impairment and Alzheimer's disease. J Alzheimers Dis. 2011; 26:59–68. [PubMed: 21593563]

van Agthoven M, Metselaar HJ, Tilanus HW, de Man RA, IJzermans JN, Martin van Ineveld BM. A comparison of the costs and effects of liver transplantation for acute and for chronic liver failure. Transpl Int. 2001; 14:87–94. [PubMed: 11370172]

Vinken M. Gap junctions and non-neoplastic liver disease. J Hepatol. 2012; 57:655–662. [PubMed: 22609308]

Vinken M, Henkens T, De Rop E, Fraczek J, Vanhaecke T, Rogiers V. Biology and pathobiology of gap junctional channels in hepatocytes. Hepatology. 2008; 47:1077–1088. [PubMed: 18058951]

Yamamoto T, Kojima T, Murata M, Takano K, Go M, Hatakeyama N, Chiba H, Sawada N. p38 MAP-kinase regulates function of gap and tight junctions during regeneration of rat hepatocytes. J Hepatol. 2005; 42:707–718. [PubMed: 15826721]

Yamaoka K, Nouchi T, Tazawa J, Hiranuma S, Marumo F, Sato C. Expression of gap junction protein connexin 32 and E-cadherin in human hepatocellular carcinoma. J Hepatol. 1995; 22:536–539. [PubMed: 7650333]

Zhang Y, He Y, Yu H, Ma F, Wu J, Zhang X. Liquiritigenin Protects Rats from Carbon Tetrachloride Induced Hepatic Injury through PGC-1α Pathway. Evid Based Complement Alternat Med. 2015; 2015:649568. [PubMed: 26199636]

Europe PMC Funders Author Manuscripts

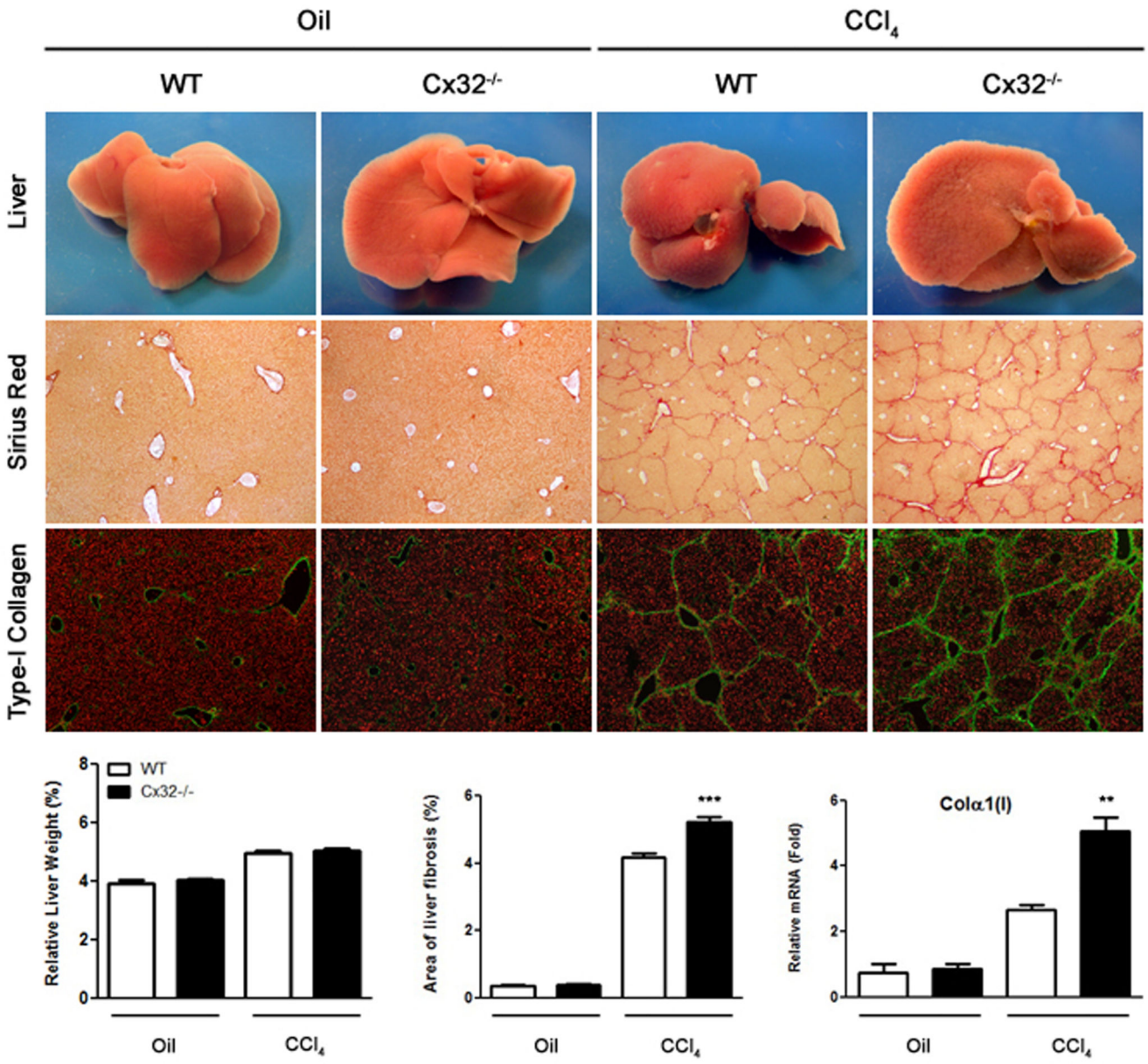

Figure 1. Loss of Cx32 enhances liver fibrosis after CCl_4-induced chronic liver injury.

Mice (n=10 *per* genotype) were administered corn oil or 10% CCl_4 ip at a gradually increased dose for 8 weeks. Liver macroscopic and relative liver weight evaluation of oil and CCl_4-treated WT and Cx32 KO mice. Fibrosis was staged by histopathological criteria (Ishak et al. 1995) and collagen morphometric analysis was performed by the quantification of the area of collagen fibers stained by Sirius red. Immunofluorescent staining of type-I collagen was performed and mRNA levels of collagen α1(I) were measured in liver tissue from oil-treated and CCl_4-treated WT and Cx32 KO mice. Magnification at 40×. Data are expressed as means ± SEM with $^{**}p < 0.01$ and $^{***}p < 0.001$ compared to WT animals.

Europe PMC Funders Author Manuscripts

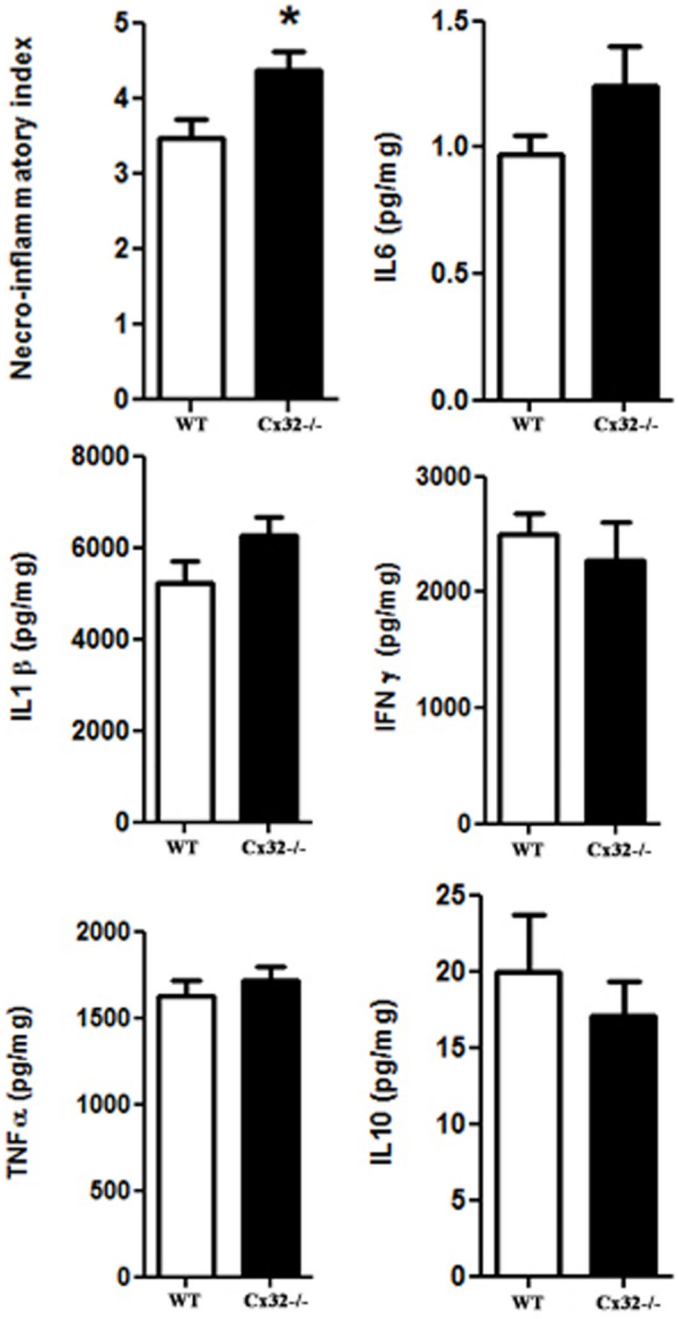

Figure 2. Loss of Cx32 enhances hepatocellular injury but does not increase the inflammatory cytokines release after CCl_4-induced chronic liver injury.

Mice (n=10 *per* genotype) were administered 10% CCl_4 ip at a gradually increased dose for 8 weeks. The histopathological liver damage was assessed by the necro-inflammatory index determined in liver sections based upon histopathological criteria (Ishak et al. 1995). The inflammatory response generated upon administration of CCl_4 leads to release of IL1β, IL6, TNFα, IFNγ, and IL10. Data are expressed as means ± SEM with $*p < 0.05$ compared to WT animals.

Europe PMC Funders Author Manuscripts

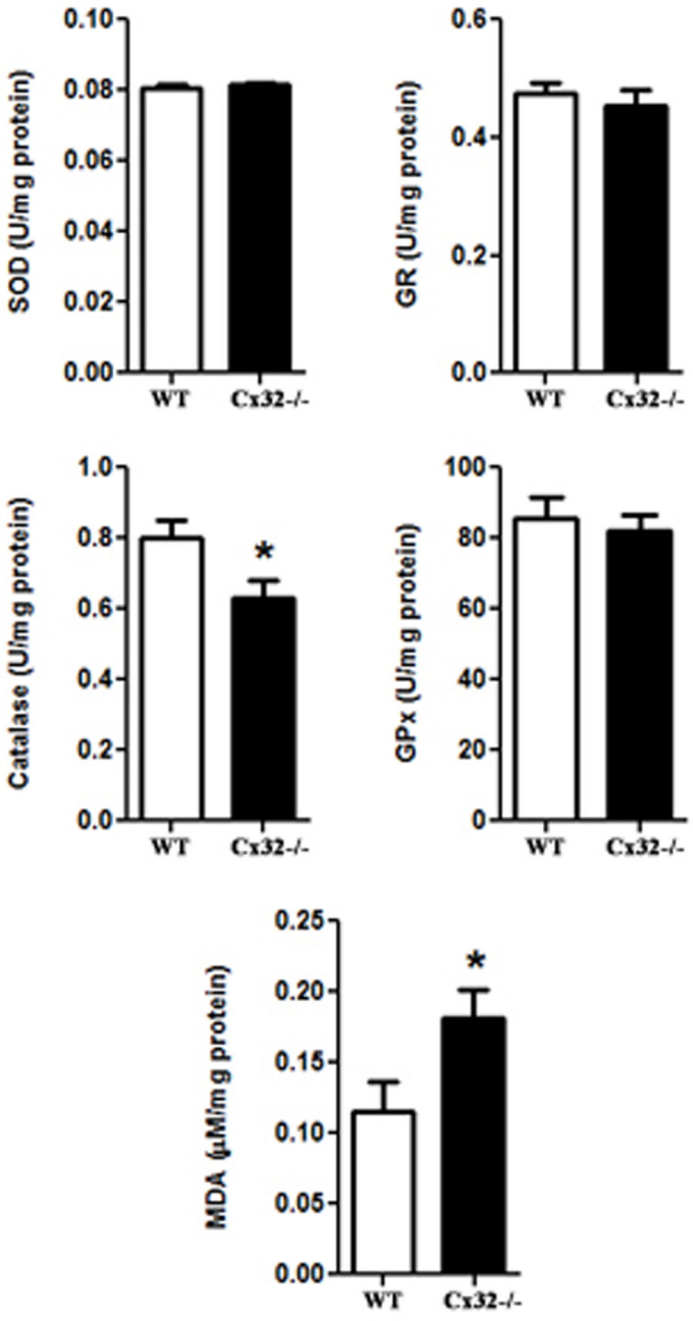

Figure 3. Loss of Cx32 enhances hepatic oxidative stress after CCl_4-induced chronic liver injury.

Mice (n=10 per genotype) were administered 10% CCl_4 ip at a gradually increased dose for 8 weeks. Anti-oxidant enzymes SOD, GR, GPx and catalase activity were determined as described in the “Methods and materials” section. Oxidative stress can compromise cellular lipids, thereby promoting the formation of MDA. Data are expressed as means ± SEM with * $p < 0.05$ compared to WT animals.

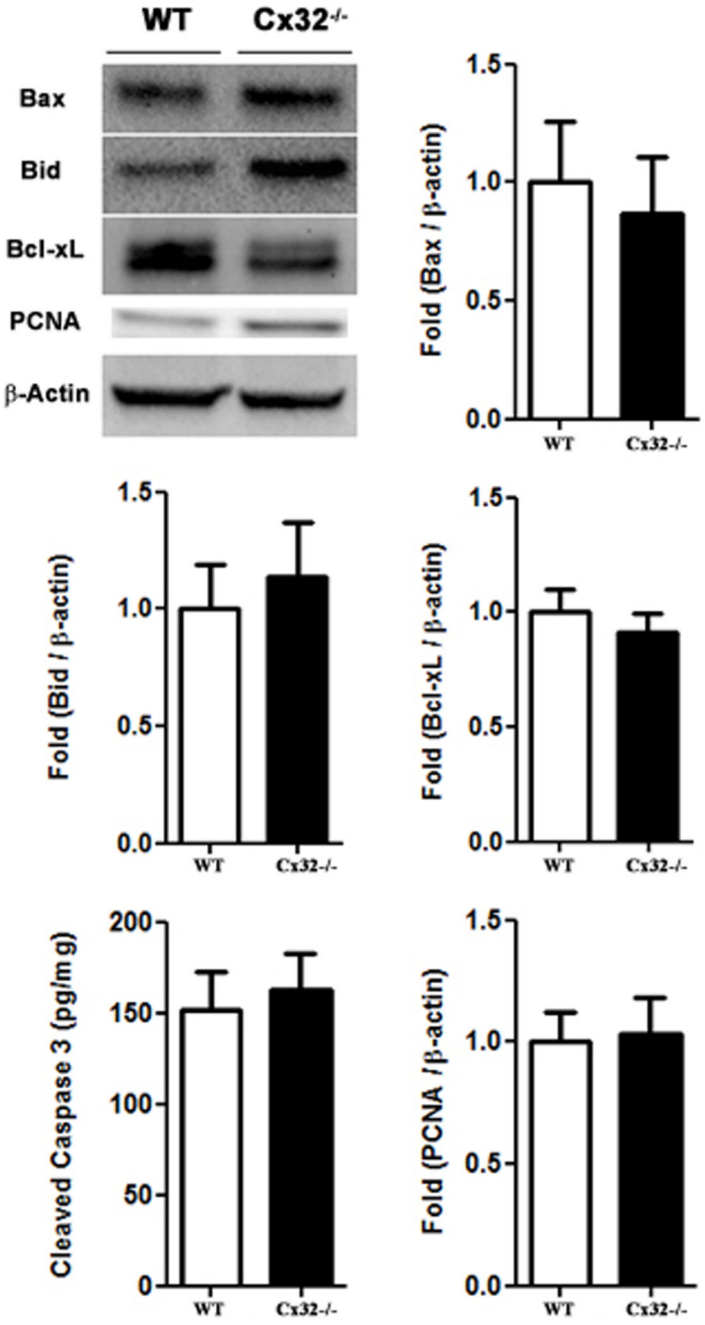

Figure 4. Loss of Cx32 does not alter the regenerative activity and the apoptotic signaling pathway after CCl_4-induced chronic liver injury.

Mice (n=10 *per* genotype) were administered or 10% CCl_4 ip at a gradually increased dose for 8 weeks. Hepatic protein levels of the pro-apoptotic Bcl-2 proteins Bax, Bid and anti-apoptotic Bcl-xl were assessed by immunoblot analysis and results were normalized against β-actin, while the pro-apoptotic cleaved caspase 3 levels were determined by ELISA (A). Liver levels of PCNA were determined by immunoblotting and normalized against β-actin (B). Data are expressed as means ± SEM.

Europe PMC Funders Author Manuscripts

Table 1

Serum biochemical parameters analyzed in WT and Cx32$^{-/-}$ mice.

Mice (n=10 per genotype) were administered corn oil or 10% CCl_4 ip at a gradually increased dose for 8 weeks. ALP, alkaline phosphatase; AST, aspartate aminotransferase; ALT, alanine aminotransferase. Data are expressed as means ± SEM with * $p < 0.05$ and ** $p < 0.01$ compared to WT animals.

Parameters	Oil		CCl_4	
	WT mice	Cx32$^{-/-}$ mice	WT mice	Cx32$^{-/-}$ mice
AST (U/L)	74 ± 1.0	71 ± 1.0	92.4 ± 4.0	117.2 ± 7.5**
ALT (U/L)	47 ± 4.2	48.5 ± 2.5	57.0 ± 3.7	68.8 ± 2.3*
ALP (U/L)	98.5 ± 7.5	96.8 ± 6.0	82.2 ± 4.5	96.9 ± 4.3
Total protein (g/dL)	5.3 ± 0.1	5.1 ± 0.2	5.3 ± 0.1	5.3 ± 0.1
Albumin (g/dL)	1.4 ± 0.2	1.1 ± 0.1	1.4 ± 0.1	1.3 ± 0.1
Total bilirrubin (mg/dL)	0.1 ± 0.1	0.1 ± 0.1	0.1 ± 0.1	0.1 ± 0.1